Supplementary Material

Rationale and Design of the PancreaSeq Panel

The PancreaSeq panel used herein was designed in part based on previously published next-generation sequencing testing results for the classification of various neoplastic pancreatic cysts, such as intraductal papillary mucinous neoplasms (IPMNs) and mucinous cystic neoplasms (MCNs), and the identification of pancreatic ductal adenocarcinomas (PDACs) reported to arise in association with mucinous cysts. For instance, mutations in *KRAS, GNAS,* and *RNF43* were included because of their high sensitivity and high specificity for mucinous cysts of the pancreas.[1–11] In rare instances, alterations in *NRAS*, *HRAS*, *BRAF,* and *STK11* have also been reported to be clinically associated with mucinous cysts.[2,5,12,13] *KRAS*, *HRAS*, *NRAS,* and *BRAF* are genes collectively known to be involved in the mitogen-activated protein kinase (MAPK) pathway. Further, the clinical utility of incorporating *TP53*, *PIK3CA*, *PTEN*, and *AKT1* testing in the setting of *KRAS* and/or *GNAS* mutations for the detection of mucinous cysts with advanced neoplasia was previously published in a prospective testing cohort but this cohort comprised only a single institutional study.[5] It is also important to note that other than *PIK3CA*, *PTEN*, and *AKT1*, genomic alterations in the remaining mammalian target of rapamycin (mTOR) genes have rarely been implicated in the molecular pathogenesis of PDAC arising from a mucinous cyst.[14–18] *SMAD4* was included because of its high prevalence in both mucinous cysts with high-grade dysplasia and PDACs associated with a mucinous cyst.[1,2,9,10,19] Specific attention to mutant allele frequencies (AFs) was made considering previously reported results of low-level variants of *TP53*, *SMAD4*, and the mTOR genes with respect to MAPK/*GNAS* alterations corresponding to an absence of advanced neoplasia.[5] However, *CDKN2A* was specifically excluded due its reported detection in both low-grade and high-grade mucinous cysts.[20]

Molecular testing of pancreatic cyst fluid is not only accurate in the identification of mucinous cysts, but also the classification of other neoplastic cysts. Genomic alterations in *VHL* have been identified in serous cystadenomas (SCAs).[1,2,5,7] Similarly, recurrent mutations in exon 3 of *CTNNB1* is highly specific for solid pseudopapillary neoplasms.[21,22] Interestingly, *CTNNB1* mutations have also been reported in mucinous cysts.[20] Mutations in *MEN1* and the mTOR genes have been detected in pancreatic neuroendocrine tumors (PanNETs), but in the absence of *KRAS* and *GNAS* mutations.[23–25] Finally, the absence of genomic alterations in the aforementioned genes is predicted to represent a non-neoplastic cyst with the consideration that false negative results may occur due to insufficient sampling of a neoplastic lesion or potentially an undescribed genomic alteration associated with a subset of pancreatic cystic neoplasms (eg, intraductal oncocytic papillary neoplasm).[26] Expected results based on previously published data are summarized in Supplementary Table 1.

Retrospective PancreaSeq Testing Cohort

The study cohort consisted of 97 endoscopic ultrasound–fine needle aspiration (EUS-FNA) obtained pancreatic cyst fluid specimens that were collected as previously published and had corresponding follow-up diagnostic surgical pathology (Supplementary Table 2). The patients ranged in age from 22 to 83 years (mean, 62.5 years; median, 63.0 years) with a slight male majority of 52%. Based on the patient's electronic medical record, associated clinical symptoms were documented for 47 (49%) patients with jaundice identified for 6 of 42 (14%) patients with a pancreatic cyst involving the head, uncinate, and/or neck. Per EUS reports, most pancreatic cysts within this cohort were seen in the body and/or tail (n = 55, 57%). Further, the pancreatic cysts ranged in size between 1.3 and 9.4 cm (mean, 3.8 cm; median, 3.2 cm) and 53 (55%) patients had a cyst >3.0 cm. Additional imaging findings included the presence of multiple cysts (n = 46, 47%), associated ductal dilation (n = 26, 27%), and a mural nodule (n = 16, 17%). On FNA, increased fluid viscosity was noted for 48 (50%) patients and an elevated CEA for 41 (42%) patients. A cytopathologic diagnosis of at least suspicious for adenocarcinoma was identified in 7 (7%) cases.

On the basis of diagnostic surgical pathology, the retrospective cohort was composed of 13 IPMN-associated adenocarcinoma, 7 IPMNs with high-grade dysplasia, 2 MCNs with high-grade dysplasia, 34 IPMNs with low-grade dysplasia, 7 MCNs with low-grade dysplasia, 9 cystic PanNETs, 2 SCAs, 16 pseudocysts, 2 lymphoepithelial cysts, 2 retention cysts, 1 acinar cell cystadenoma, 1 epidermoid cyst within an intrapancreatic spleen, and 1 squamous cyst of the pancreas. The sensitivity and specificity of MAPK/*GNAS* alterations for a mucinous cyst was 89% and 100%, respectively. In comparison, increased fluid viscosity and an elevated CEA had lower sensitivities (68% and 56%, respectively) and lower specificities (85% and 82%, respectively). In conjunction with MAPK/*GNAS* mutations, alterations in *TP53, SMAD4*, and/or the mTOR genes had 86% sensitivity and 96% specificity for a mucinous cyst with advanced neoplasia. The sensitivities and specificities of individual genomic combinations for advanced neoplasia were as follows: MAPK/*GNAS* and *TP53* alterations were associated with 64% sensitivity and 99% specificity; MAPK/*GNAS* and *SMAD4* alterations were associated with 46% sensitivity and 100% specificity; and MAPK/*GNAS* and mTOR alterations were associated with 32% sensitivity and 96% specificity. Of note, the combination of MAPK/*GNAS* with *TP53* and/or *SMAD4* yielded a sensitivity of 77% and a specificity of 99%. However, on exclusion of low-level *TP53* and *PIK3CA* mutations, the sensitivity and specificity of the MAPK/*GNAS* and *TP53*, *SMAD4,* and/or mTOR gene combination of genomic alterations was 86% and 100%, respectively. The sensitivities and specificities for advanced neoplasia were lower for the presence of associated clinical symptoms (55% and 53%), jaundice for pancreatic head cysts (20% and 89%), cyst size of >3.0 cm (59% and 47%), main pancreatic duct dilatation (45% and 79%), a mural

nodule (27% and 87%), and a cytopathologic diagnosis of at least suspicious for adenocarcinoma (27% and 99%).

Prospective PancreaSeq Testing Cohort

In total, 1993 EUS-FNA–obtained pancreatic cyst fluid specimens from 1889 patients were prospectively analyzed for genomic alterations over a 2-year time frame. Among these cases, 1887 (98%) specimens from 1832 patients were satisfactory for PancreaSeq testing (Supplementary Table 3). The DNA concentration from these specimens ranged between 0.01 and 283 ng/μL (mean, 6.84 ng/μL; median, 4.4 ng/μL). This patient cohort was predominantly female (n = 1048, 56%) and ranged in age from 12 to 80 years (mean, 66.3 years; median, 69.0 years). Associated clinical and imaging data were available for most patients with documentation of associated clinical symptoms (n = 1227, 67%), jaundice for pancreatic head/uncinate/neck cysts (n = 635, 34%), pancreatic cyst location (n = 1225, 65%), pancreatic cyst size (n = 1167, 62%), changes in cyst size (n = 434, 23%), the presence of multiple cysts (n = 1167, 62%), main duct dilatation (n = 1166, 62%), and a mural nodule (n = 1174, 62%). Further, on FNA, increased fluid viscosity by string sign assessment (n = 1119, 59%), pancreatic cyst fluid CEA (n = 712, 38%), and cytopathologic evaluation (n = 642, 34%). Genomic alterations in *KRAS*, *GNAS*, *BRAF*, *VHL*, *TP53*, *SMAD4*, *CTNNB1*, and the mTOR genes and their clinicopathologic correlative findings are summarized in Supplementary Tables 5, 6, and 7.

PancreaSeq Testing of PanNETs

With respect to PancreaSeq testing, a clinicopathologic analysis of cystic (n = 34, 39%) and solid (n = 53, 61%) PanNETs was performed for 87 preoperative specimens (Supplementary Table 8). This study cohort consisted of an equivalent number of female-to-male patients who ranged in age between 25 and 85 years (mean, 61.2 years; median, 65.0 years). PanNETs were predominantly located within the body and/or tail of the pancreas (n = 53, 61%) and ranged in size from 1.0 to 9.3 cm (mean, 2.7 cm; median, 2.2 cm). Most PanNETs were >2.0 cm in greatest dimension (n = 49, 56%). Available surgical pathologic data and follow-up included WHO grade (based on Ki-67 and mitotic index) (n = 84), lymphovascular invasion (n = 82), perineural invasion (n = 82), clinical/pathologic (c/p) T-stage (n = 82), N-stage (n = 82), ATRX/DAXX immunohistochemical expression (n = 84), telomere-specific fluorescence in situ hybridization data to assess for alternative lengthening of telomeres (ALT) (n = 84), and distant metastasis (n = 84).

Comparative Whole Transcriptome (RNA) Sequencing of BRAF-Mutant and KRAS-Mutant IPMNs With Low-Grade Dysplasia

Whole transcriptome (RNA) sequencing and differential gene expression analysis was performed for 18 *GNAS*-mutant, diagnostically confirmed IPMNs with low-grade dysplasia and co-occurring mutations in either *BRAF* (n = 9) or *KRAS* (n = 9). For each cohort, cases consisted of 3 preoperative EUS-FNA specimens and 6 surgical resection specimens obtained from the prospective PancreaSeq testing cohort (Supplementary Figure 4). Although a comparison of *BRAF*-mutant and *KRAS*-mutant IPMNs identified a trend in the differential expression of TERT and SCARNA1, no statistically significant difference was identified. Overall, *BRAF*-mutant and *KRAS*-mutant IPMNs with low-grade dysplasia that also harbored a *GNAS* mutation demonstrated similar gene expression profiles.

Supplementary References

1. Springer S, Wang Y, Molin MD, et al. A combination of molecular markers and clinical features improve the classification of pancreatic cysts. Gastroenterology 2015;149:1501–1510.
2. Springer S, Masica DL, Dal Molin M, et al. A multimodality test to guide the management of patients with a pancreatic cyst. Sci Transl Med 2019;11:eaav4772.
3. Singhi AD, Zeh HJ, Brand RE, et al. American Gastroenterological Association guidelines are inaccurate in detecting pancreatic cysts with advanced neoplasia: a clinicopathologic study of 225 patients with supporting molecular data. Gastrointest Endosc 2016; 83:1107–1117.e2.
4. Nikiforova MN, Khalid A, Fasanella KE, et al. Integration of KRAS testing in the diagnosis of pancreatic cystic lesions: a clinical experience of 618 pancreatic cysts. Mod Pathol 2013;26:1478–1487.
5. Singhi AD, McGrath K, Brand RE, et al. Preoperative next-generation sequencing of pancreatic cyst fluid is highly accurate in cyst classification and detection of advanced neoplasia. Gut 2018;67:2131–2141.
6. Singhi AD, Nikiforova MN, Fasanella KE, et al. Preoperative GNAS and KRAS testing in the diagnosis of pancreatic mucinous cysts. Clin Cancer Res 2014; 20:4381–4389.
7. Wu J, Jiao Y, Dal Molin M, et al. Whole-exome sequencing of neoplastic cysts of the pancreas reveals recurrent mutations in components of ubiquitin-dependent pathways. Proc Natl Acad Sci U S A 2011; 108:21188–21193.
8. Wu J, Matthaei H, Maitra A, et al. Recurrent GNAS mutations define an unexpected pathway for pancreatic cyst development. Sci Transl Med 2011;3:92ra66.
9. Jones M, Zheng Z, Wang J, et al. Impact of next-generation sequencing on the clinical diagnosis of pancreatic cysts. Gastrointest Endosc 2016;83:140–148.
10. Rosenbaum MW, Jones M, Dudley JC, et al. Next-generation sequencing adds value to the preoperative diagnosis of pancreatic cysts. Cancer Cytopathol 2017;125:41–47.
11. Fischer CG, Beleva Guthrie V, Braxton AM, et al. Intraductal papillary mucinous neoplasms arise from multiple independent clones, each with distinct mutations. Gastroenterology 2019;157:1123–1137.e22.
12. Sahin F, Maitra A, Argani P, et al. Loss of Stk11/Lkb1 expression in pancreatic and biliary neoplasms. Mod Pathol 2003;16:686–691.

13. Sato N, Rosty C, Jansen M, et al. STK11/LKB1 Peutz-Jeghers gene inactivation in intraductal papillary-mucinous neoplasms of the pancreas. Am J Pathol 2001;159:2017–2022.
14. Garcia-Carracedo D, Chen ZM, Qiu W, et al. PIK3CA mutations in mucinous cystic neoplasms of the pancreas. Pancreas 2014;43:245–249.
15. Bruckman KC, Schonleben F, Qiu W, et al. Mutational analyses of the BRAF, KRAS, and PIK3CA genes in oral squamous cell carcinoma. Oral Surg Oral Med Oral Pathol Oral Radiol Endod 2010;110:632–637.
16. Schonleben F, Qiu W, Allendorf JD, et al. Molecular analysis of PIK3CA, BRAF, and RAS oncogenes in periampullary and ampullary adenomas and carcinomas. J Gastrointest Surg 2009;13:1510–1516.
17. Schonleben F, Qiu W, Remotti HE, et al. PIK3CA, KRAS, and BRAF mutations in intraductal papillary mucinous neoplasm/carcinoma (IPMN/C) of the pancreas. Langenbecks Arch Surg 2008;393:289–296.
18. Schonleben F, Qiu W, Ciau NT, et al. PIK3CA mutations in intraductal papillary mucinous neoplasm/carcinoma of the pancreas. Clin Cancer Res 2006;12:3851–3855.
19. Noe M, Niknafs N, Fischer CG, et al. Genomic characterization of malignant progression in neoplastic pancreatic cysts. Nat Commun 2020;11:4085.
20. Amato E, Molin MD, Mafficini A, et al. Targeted next-generation sequencing of cancer genes dissects the molecular profiles of intraductal papillary neoplasms of the pancreas. J Pathol 2014;233:217–227.
21. Abraham SC, Klimstra DS, Wilentz RE, et al. Solid-pseudopapillary tumors of the pancreas are genetically distinct from pancreatic ductal adenocarcinomas and almost always harbor beta-catenin mutations. Am J Pathol 2002;160:1361–1369.
22. Selenica P, Raj N, Kumar R, et al. Solid pseudopapillary neoplasms of the pancreas are dependent on the Wnt pathway. Mol Oncol 2019;13:1684–1692.
23. Heaphy CM, de Wilde RF, Jiao Y, et al. Altered telomeres in tumors with ATRX and DAXX mutations. Science 2011;333:425.
24. Jiao Y, Shi C, Edil BH, et al. DAXX/ATRX, MEN1, and mTOR pathway genes are frequently altered in pancreatic neuroendocrine tumors. Science 2011;331:1199–1203.
25. Scarpa A, Chang DK, Nones K, et al. Whole-genome landscape of pancreatic neuroendocrine tumours. Nature 2017;543:65–71.
26. Singhi AD, Wood LD, Parks E, et al. Recurrent rearrangements in PRKACA and PRKACB in intraductal oncocytic papillary neoplasms of the pancreas and bile duct. Gastroenterology 2020;158:573–582.e2.

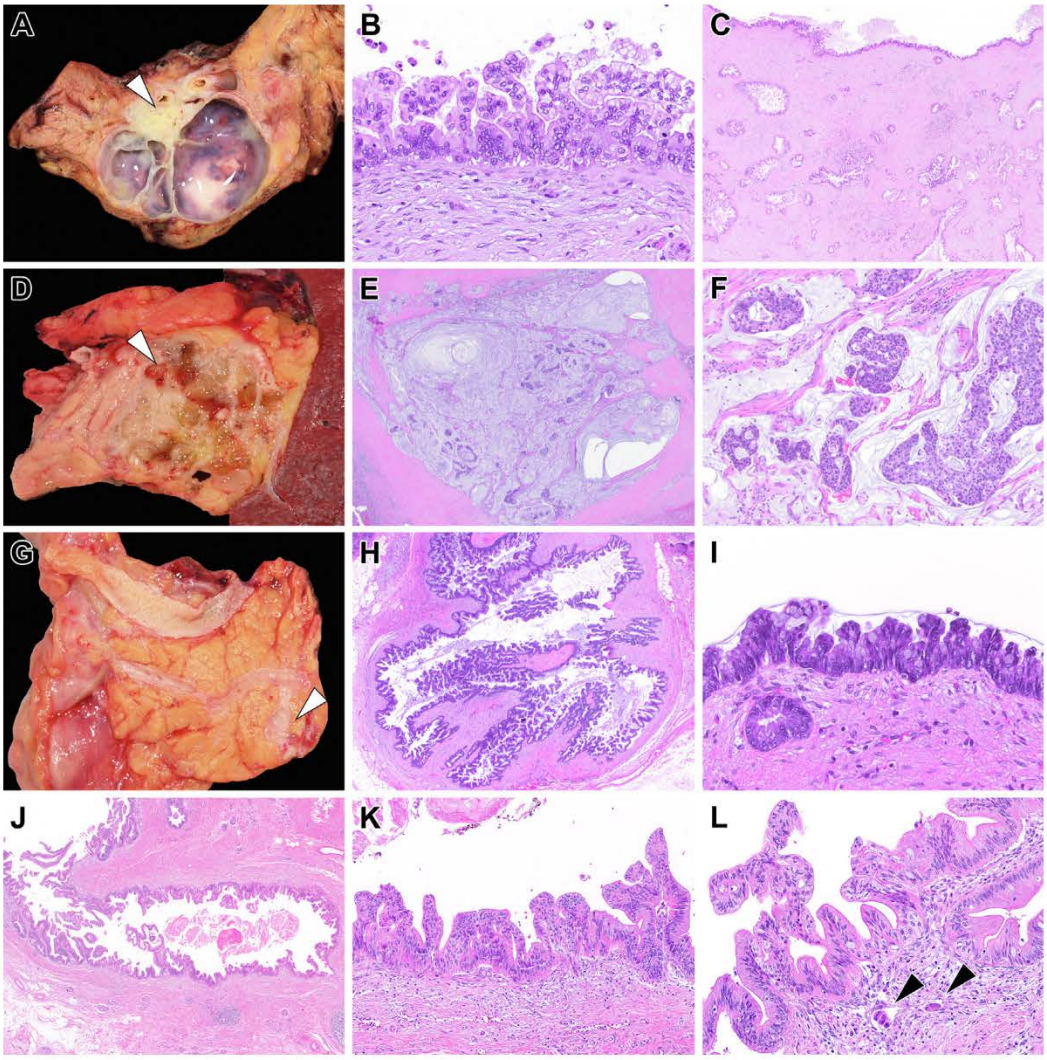

Supplementary Figure 1. Representative examples of diagnostic surgical pathology for IPMNs with advanced neoplasia that had preoperative PancreaSeq testing. (*A*) An IPMN-associated PDAC (*white arrowhead*) in a patient had PancreaSeq testing 1 year prior. One-year prior, other than a 3.1-cm pancreatic cyst, no concerning preoperative clinical, imaging, or preoperative pathologic findings were identified. However, PancreaSeq testing revealed *KRAS* and *GNAS* mutations along with LOH for *RNF43* and *TP53*. The patient deferred surgery and on imaging follow-up a solid lesion was identified and corresponded to (*B* and *C*) a moderately differentiated PDAC in association with an IPMN with extensive high-grade dysplasia. (*D*) A 3.5-cm pancreatic tail cyst (*white arrowhead*) with otherwise no concerning preoperative clinical, imaging, or preoperative pathology findings. Cytopathologic evaluation of EUS-FNA pancreatic cyst fluid only detected acellular mucin, but PancreaSeq testing identified a *KRAS* mutation and LOH for *RNF43* and *TP53*. (*E* and *F*) Microscopically, a colloid carcinoma was identified arising in IPMN. (*G*) A 1.2 cm branch-duct IPMN (*white arrowhead*) with focal ductal dilation, and otherwise no concerning preoperative clinical, imaging, or preoperative pathologic findings; however, PancreaSeq testing revealed mutations in *KRAS, GNAS,* and *CTNNB1* of similar AFs. (*H* and *I*) Histopathologic examination revealed an IPMN with extensive high-grade dysplasia. (*J*) A branch-duct IPMN no concerning preoperative clinical, imaging, or preoperative pathologic findings. PancreaSeq testing, however, detected *KRAS* and *GNAS* mutations and LOH for *SMAD4*. (*K* and *L*) On surgical resection, a small (<0.1 cm), microscopic PDAC (*white arrowheads*) composed of single cells was identified in association with an IPMN with high-grade dysplasia.

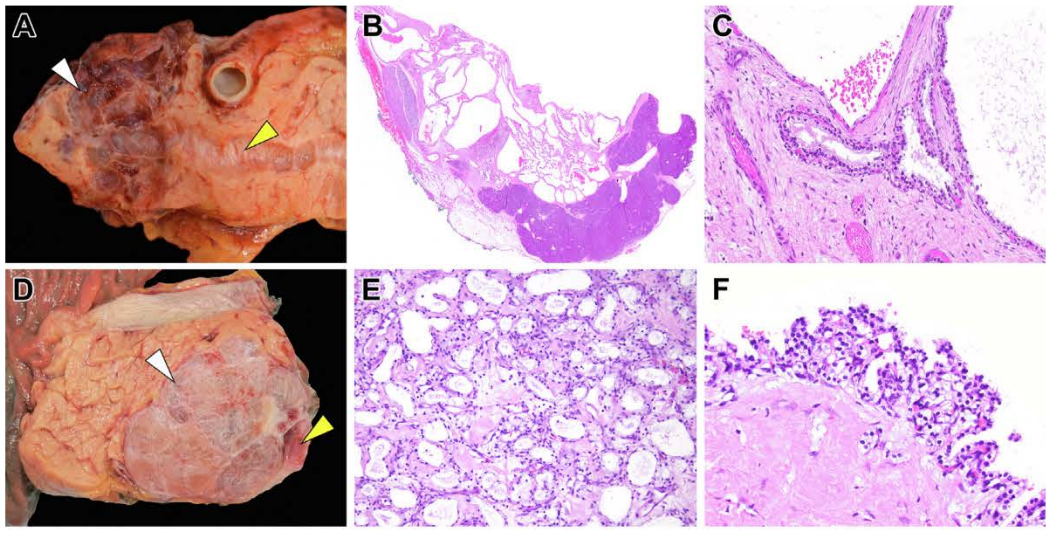

Supplementary Figure 2. SCAs were not only characterized by *VHL* alterations, but also *TP53* and *TERT* promoter mutations. (*A*) A 3.8-cm SCA (*white arrowhead*) of the pancreatic body that was surgically resected due to secondary obstruction of the main pancreatic duct (*yellow arrowhead*). Preoperative PancreaSeq testing revealed *VHL* and *TP53* alterations. (*B* and *C*) Microscopically, the SCA consisted of a multilocular cyst that was lined by glycogen-laden epithelium. (*D*) An 8.0-cm SCA (*white arrowhead*) of the pancreatic head was resected due to main pancreatic ductal obstruction (*yellow arrowhead*) resulting in the patient presenting with chronic pancreatitic symptoms. Preoperative PancreaSeq testing detected *VHL* and *TERT* promoter mutations. (*E* and *F*) The corresponding diagnostic surgical pathology showed a microcystic growth pattern and multiple foci of pseudopapillae of glycogen-laden epithelium.

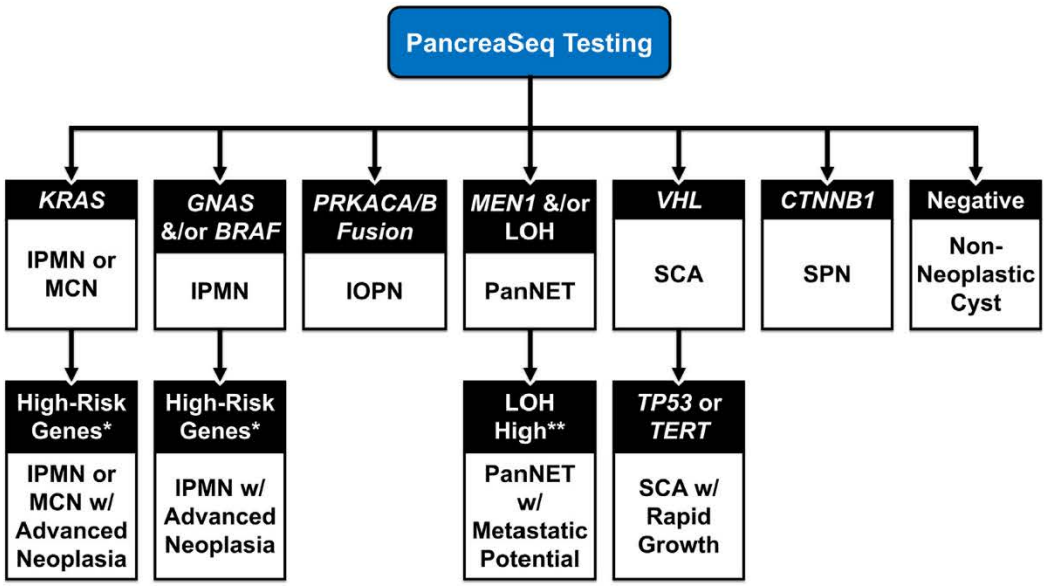

Supplementary Figure 3. Algorithmic approach to key genomic alterations detected by PancreaSeq testing and their clinical significance. *Refers to high-risk genes that include genomic alterations in TP53, SMAD4, CTNNB1, and the mTOR genes, and **refers to LOH of $\geq$3 genes.

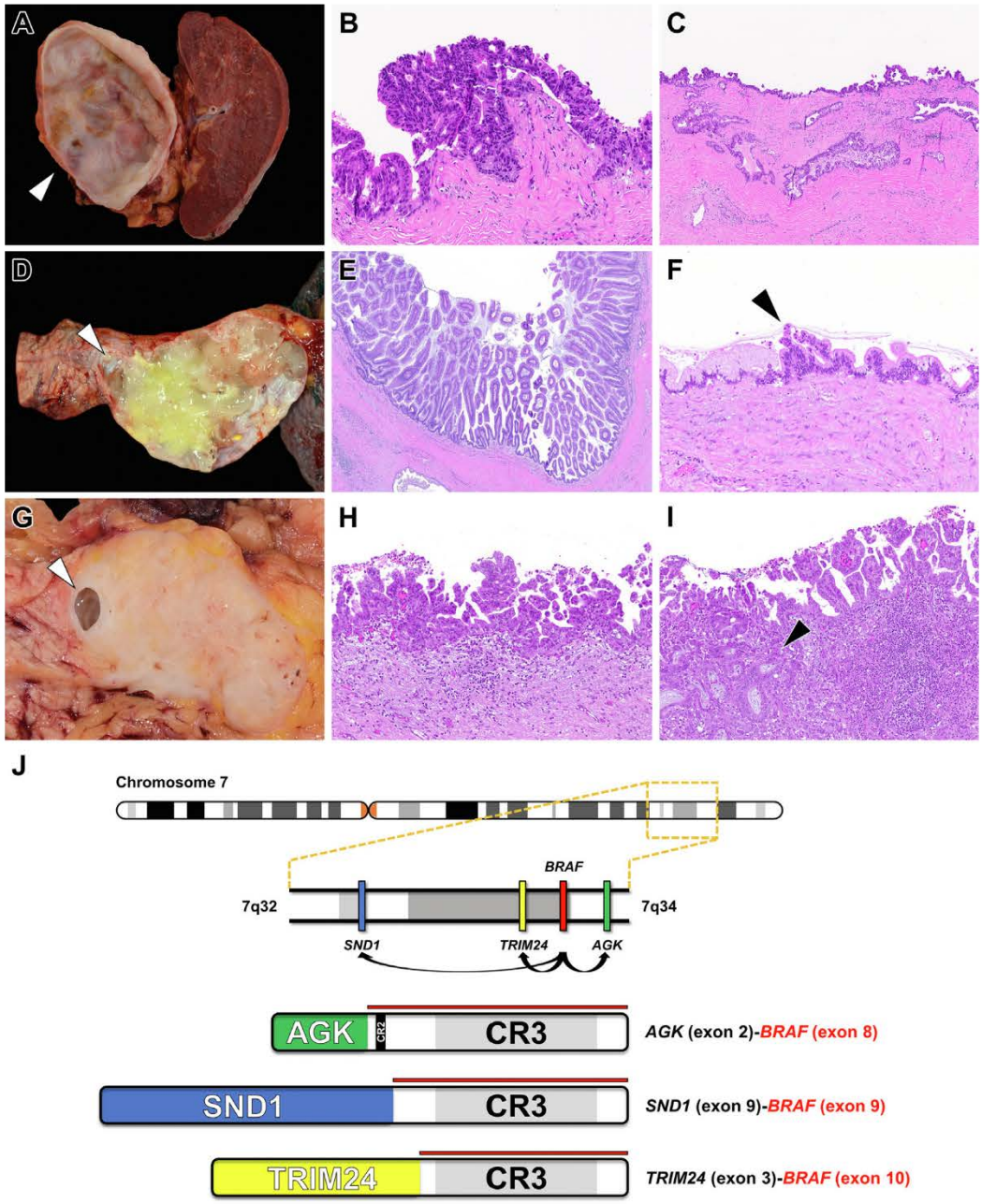

Supplementary Figure 4. Several IPMNs were negative for MAPK mutations by PancreaSeq testing. However, expanded molecular (Oncomine) testing identified alterative MAPK driver mutations for 5 cases. (*A*) An 8.3-cm pancreatic body/tail IPMN (*white arrowhead*) with (*B*) extensive high-grade dysplasia and (*C*) focal invasive PDAC. Oncomine testing detected an *ERBB2* amplification. In addition to *ERBB2*, 4 IPMNs were found to harbor *BRAF* fusion genes. (*D*) A 4.9-cm pancreatic body/tail IPMN (*white arrowhead*) that on preoperative PancreaSeq testing revealed a *GNAS* mutation and LOH for *RNF43* and *TP53*. (*E* and *F*) Microscopically, the IPMN with characterized by papillary and flat architecture, and multiple foci of high-grade dysplasia (*black arrowhead*). Postoperative Oncomine testing of the IPMN found an AGK-BRAF fusion gene. (*G*) A 2.7-cm pancreatic head/uncinate IPMN (*white arrowhead*) was surgically resected due to the detection of a mural nodule and subsequent malignant cytopathology. While preoperative PancreaSeq testing identified *GNAS* and *TP53* mutations of similar AFs, no *KRAS* or *BRAF* mutations were seen. (*H* and *I*) The corresponding surgical pathology was consistent with an IPMN-associated PDAC (*black arrowhead*). In addition, postoperative Oncomine testing showed the presence of an SND1-BRAF fusion gene. (*J*) A total of 4 IPMNs were found to harbor *BRAF* fusion genes and consisted of *AGK* (exon 2)-*BRAF* (exon 8) (n = 1), *SND1* (exon 9)-*BRAF* (exon 9) (n = 2), and *TRIM24* (exon 3)-*BRAF* (exon 10) (n = 1).

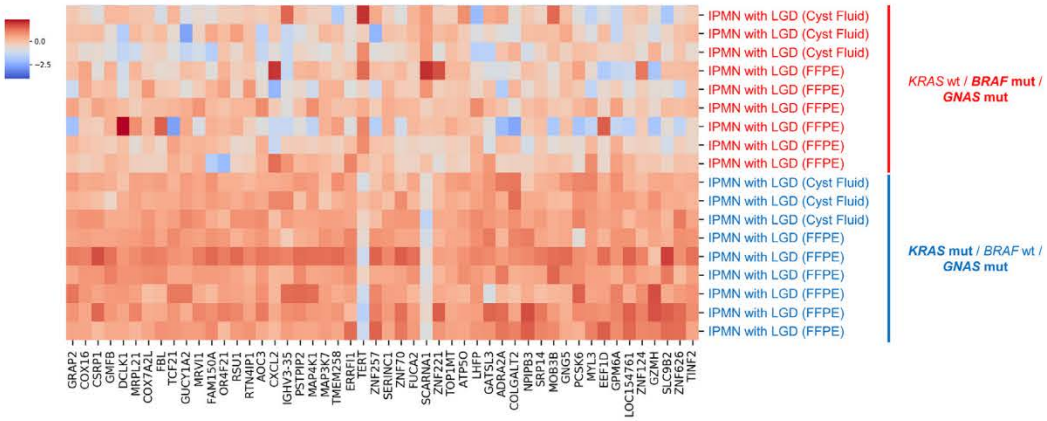

Supplementary Figure 5. Differential gene expression analysis was performed for 18 *GNAS*-mutant IPMNs with low-grade dysplasia and co-occurring mutations in either *BRAF* (n = 9) or *KRAS* (n = 9). A trend toward increased expression of TERT and SCARNA1 was identified in *BRAF*-mutant IPMNs as compared with *KRAS*-mutant IPMNs. However, these findings were not statistically significant. Overall, *BRAF*-mutant and *KRAS*-mutant IPMNs with low-grade dysplasia and *GNAS* mutations demonstrated similar gene expression profiles.